



The design of DC micro grid with a load-based battery discharge method for remote island electrification utilizes marine currents and solar photovoltaic

Faanzir^{1,2}, Mochamad Ashari^{1*}, Soedibyo¹, Suwito¹, Umar²

Department of Electrical Engineering, Institut Teknologi Sepuluh Nopember, Surabaya, Indonesia
Department of Electrical Engineering, Universitas Khairun, Ternate, Indonesia

Article Info

Keywords:

Battery, Discharge, Direct current, Marine Current, Solar Photovoltaic

Article history:

Received: October 21, 2022

Accepted: November 03, 2022

Published: November 30, 2022

Cite:

Faanzir, M. . Ashari, Soedibyo, Suwito, and Umar, "The Design of DC Micro Grid with a Load-Based Battery Discharge Method for Remote Island Electrification Utilizes Marine Currents and Solar Photovoltaic", *KINETIK*, vol. 7, no. 4, Nov. 2022.
<https://doi.org/10.22219/kinetik.v7i4.1576>

*Corresponding author.

Faansir

E-mail address:

Anzir_unkhair@yahoo.co.id

Abstract

This paper presents the design of DC micro grid with a load-based battery discharge method for remote island electrification utilising marine currents and solar photovoltaic. To anticipate the intermittent, a load-based battery discharge method is proposed. A centralized battery storage is sized according to the unfilled load demand by the marine current and the solar PV. Thus, the length of the turbine diameter is varied to meet the optimum system size. Hourly data of marine current speed from Cibalulu Strait in Maluku, Indonesia is provided. Data at a typical time, shows that the marine current peak power occurs every 6 hours perday, whereas the PV is at noon. The loads divide into 6 categories, including household 1, household 2, villagse office, school, mosque, and public health center with the peak demand as 112 kW and 856 kWh perday. All loads, mainly for lightings and electronic equipment work in 24 V DC through converters. The distribution network employs 320 V DC connecting from the power plan to the community residents. Simulations demonstrate that the battery size, solar PV, and turbine radius matches to meet the loads. Simulations also show that the battery utilization meets its current and capacity, meaning that an optimum size and filling the load profile can be smoothly conducted.

1. Introduction

The development of green electricity supply for rural and remote places has become a high priority in recent decades, following the world program of the Sustainable Development Goals (SDG). To provide electricity in rural areas, diesel generators are commonly used because of their easy and instant installation, but they are expensive in the operation costs and generate emissions [1]. Other renewable energy sources include wind, solar power, marine/ ocean currents, and waves [2], [3]. The marine current is an ideal power plant for small islands, typically with the strait. It provides a high power of energy, easy to convert, and abundant.

Problems face the power system utilizing a marine current generator include the intermittent characteristics of the current flow. The marine current of the system study, which is located in Capalulu Strait, Maluku - Indonesia, meets the peak speed in every 6-hour within 24 hours. This causes an unfilled of load profiles by the source power.

Researchers have proposed hybrid systems to eliminate the intermittent problems [4]. A wind turbine may be attached to form a hybrid energy system [5]. But, wind speed at the location may be weak and need a huge construction to cover the load. Wind speed may also have unpredictable of supply during the entire year [6]. Another configuration is a marine current and solar PV hybrid system [7]. The marine generator combined with the solar PV may fill the load profiles during the day. However, when the speed of marine current reaches low during the night, the system may be lack of power. Therefore, a battery storage is needed to meet the rest of unfilled load profile by the marine current and the solar PV [8].

In order to improve the hybrid system efficiency and performances, selection of the battery parameters, the battery placement, and the distribution network voltage is considered. The battery bank is included in the DC bus to absorb excess power and discharge it when necessary. The battery attributes are evaluated based on the applied parameters. These important parameters include the maximum amount of energy that can be stored discharge rate, nominal voltage, battery capacity, battery life, number of cycles, and temperature [9]. The placement of battery banks in renewable energy systems is generally centralized near the energy sources. This makes the maintenance and monitoring easier. However, this method requires additional battery room, investment costs, and maintenance personnel, which will be charged to the customer evenly. Centralized batteries also lose more power in the distribution network. if one battery is damaged, it disrupts the whole system.

Distributed battery placement has several advantages. The battery releases energy according to the load required, and the power losses due to the distribution network are smaller. When battery damage occurs in certain

locations, it does not affect other locations. Distributed batteries do not require battery room investment and maintenance costs. The existence of IoT-based technology makes controlling and monitoring distributed batteries easy.

Small island communities commonly use electricity for lightings and supplying electronic loads, such as radio, charging mobile phones, etc. A dc micro-grid becomes a suitable system for this typical community. The renewable sources generate dc voltage, the distribution network applies dc voltage, and the housing system uses dc voltage. Due to avoiding conversion of energy, the system efficiency is improved [10]. Adopting a DC home offers many benefits, such as energy savings due to higher efficiency, minimum environmental costs, and more effective use of equipment [11].

This study presents optimization and sizing design of a DC micro-grid utilizing marine current/ solar PV/ battery hybrid system. It employs a load-based battery discharge method, which varies the turbine diameter, the solar PV power, and battery capacity to meet the minimum cost of the system. A data set consisting of hourly marine current speed for a typical year is provided. Simulations were conducted based on a typical day and month, considering the minimum and maximum speeds, to represent the entire year marine current.

2. Modelling the System Study

Figure 1 depicts the entire system study. The system uses two renewable energy sources, such as solar arrays and marine current generators. Both include converters to connect to the 380 V dc bus. A centralized battery storage system is used, and the dc-to-dc converter regulates the battery voltage and charge-discharge cycles. When the sources are insufficient, the battery also serves as a backup power source. The load voltage is 24 V dc, while the dc bus is 320 V. In this research, where communities live in a remote small island employs six different customer types: household 1, household 2, village, office, school, mosque, and public health center. The daily energy requirement is 856 kWh, with the peak load demand being 112 kW and the average power being 36 kW.

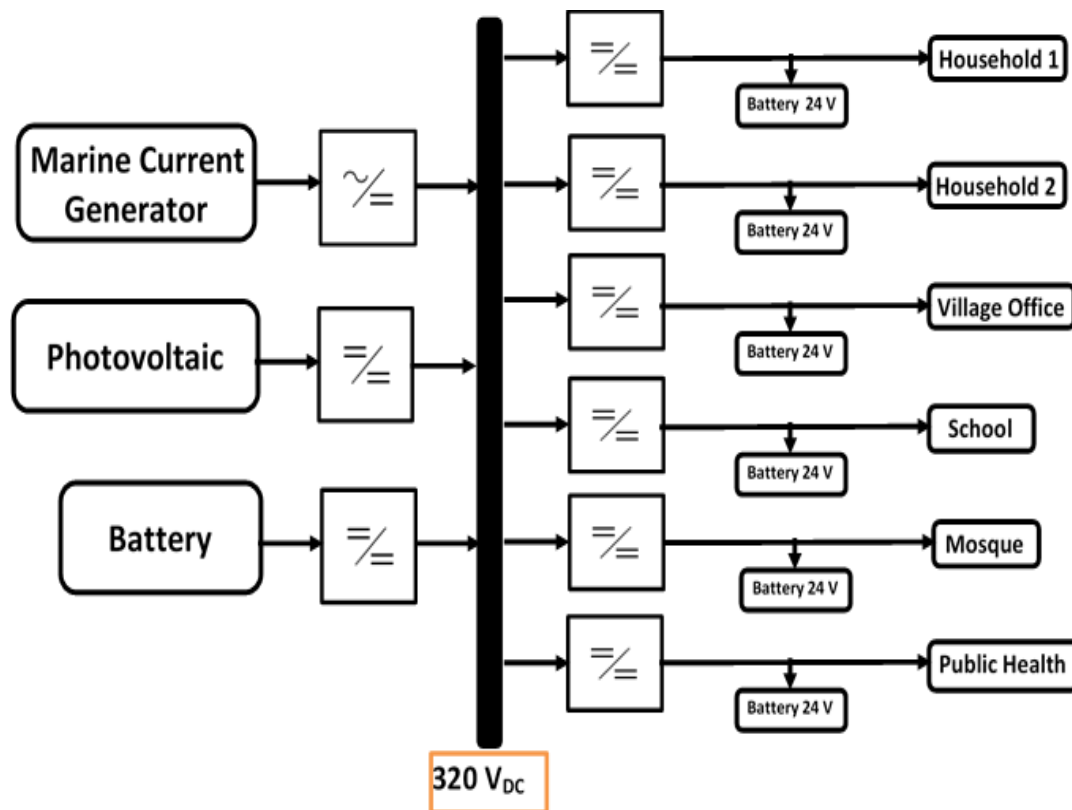


Figure 1. The Configuration of the Proposed System

2.1 Load Characteristics

Dofa Village is one of the settlements near the Capalulu Strait where the system is located. 400 people live in this village, which also has two schools, a village office, a mosque, and a community health center. With 230 pieces, Household 1 is a straightforward and compact form. With 170 units, the households 2 is a larger variety. The equipment utilized each day is used to compute the power load demand for each kind. The resistance (R) of the dc electrical equipment is displayed in Table 1.

Table 1. List of Appliances

Appliances	Volt	Watt	R (Ohm)
Led	12	5	28.8
Fan	12	30	4.8
Television	12	60	2.4
Mobile phone	12	14	10.28
Laptop	12	45	3.2
Water pump	12	80	1.8
Medical tools	12	150	0.96

Table 2 lists the number of appliances for each consumer type. Each appliance's energy requirement is also shown. The household 2 has the largest daily energy consumption at 441.32 kWh. The mosque has the lowest energy usage at 23.76 kWh, mostly for lighting, fans, a water pump, and a sound system. Within a 24-hour period, the hamlet will use 856.1 kWh in total.

Figure 2 displays the load profile for the entire community. The load profile for each customer type is also shown. The following diagram illustrates how the load power and energy demand were calculated. The power on each piece of equipment and the number of pieces of equipment (n) used determine the total amount of power used by the customer (P_L) Equation 1.

$$P_L(W) = n \cdot P_{unit} \tag{1}$$

While E_L is equal to the electric power from equation (1) times the operating time of equipment (t) as follows Equation 2.

$$E_L(Wh) = P_L \cdot t \tag{2}$$

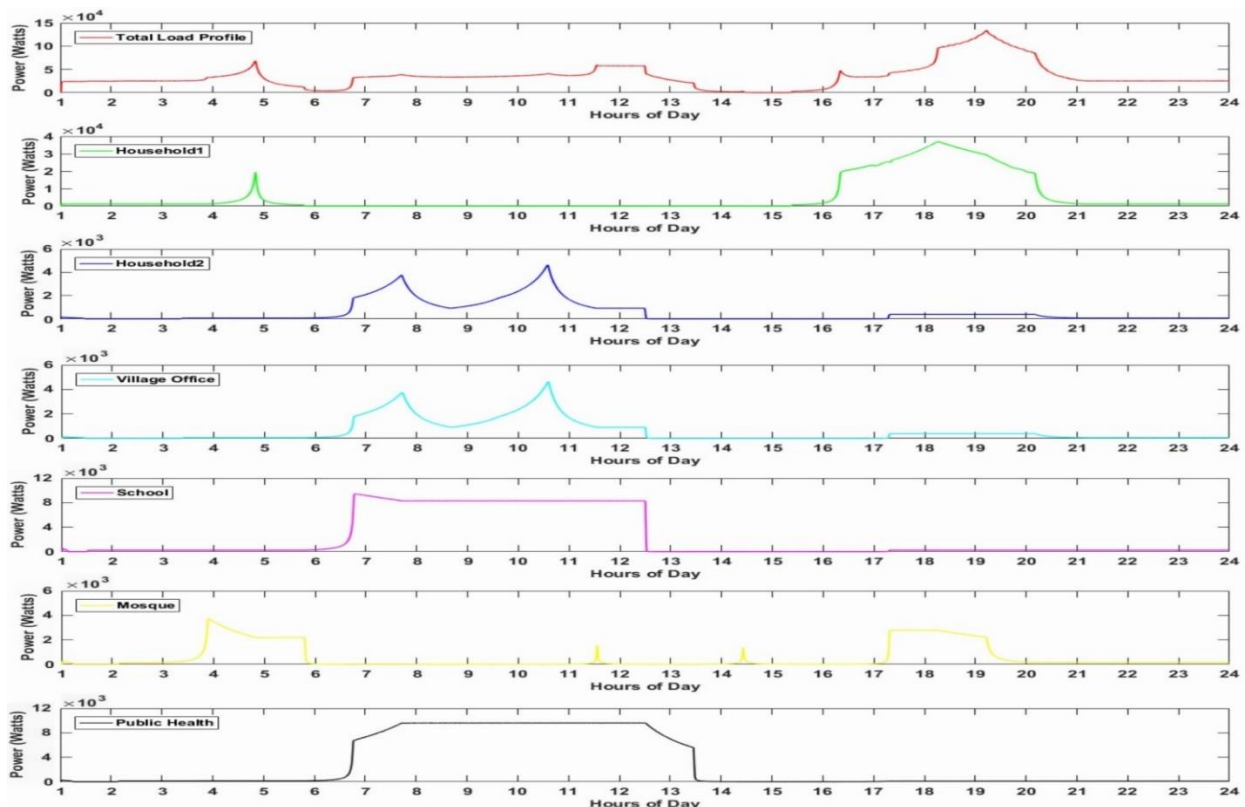


Figure 2. Total Load Profile and Each Customer Category

For a 24-hour period, the energy demand (kWh) and the load profile (kW) are provided in hourly data. Table 2 lists the number of appliances for each consumer type. Each appliance's energy demand is also shown in the Table 2. The household 2 has the greatest daily energy consumption at 441.32 kWh. The mosque has the lowest energy usage

412 Kinetik: Game Technology, Information System, Computer Network, Computing, Electronics, and Control
 at 23.76 kWh, mostly for lighting, fans, a water pump, and a sound system. The village needs 856.1 kWh of electricity in total per 24 hours.

Table 2. The Total Electrical Energy Consumed by Each Type of Customer.

Customer	Total	Number of appliances								Energy Total (kWh)
		Led	Fan	TV	Phone	Laptop	Water pump	Sound System	Medical tool	
Household1	230	3	1	1	1	1	1	0	0	240.58
Household2	170	10	3	2	4	2	1	0	0	441.32
Village Office	1	6	2	1	5	5	1	0	0	26.22
School	2	6	2	1	7	6	1	0	0	58.37
Mosque	1	10	4	0	0	0	1	1	0	23.76
Public Health	1	7	3	1	5	5	1	0	3	65.88

2.2 The Distribution System

Marine currents generate electricity through the operation of a turbine connected to an AC generator. The electricity is converted into dc system using an AC-to-DC converter [12] [13]. Solar PV also requires a DC converter to regulate the dc output voltage [14]. Both generators produce DC electricity, which is fed into the DC bus and then a battery bank is connected to it through a charge controller. The system configuration is shown in Figure 1. Batteries are charged and used in accordance with load using a buck converter. A buck converter can reduce the bus voltage to the battery's operating voltage [15] [16].

Each piece of equipment used in this investigation is powered by direct current (DC) voltage. A small battery in the load may be applied to smooth the voltage. But, the proposed system assumes without small battery, since the function is covered by capacitor inside the buck converter. The primary factor in selecting a DC-based power system is that it offers enticing benefits in terms of ease of use, low cost, and efficiency [17].

3. Sources characteristic

The battery and the loads are supplied with electricity by two different power sources: a marine current generator and solar photovoltaics.

3.1 Marine Current Generator

Using a turbine, marine current is able to capture energy from the underwater current flow [18]. To generate electricity, a generator is connected. A wind turbine's properties and formula are comparable. Since the quantity of power generated relies on the magnitude of the current speed as well as the size and kind of turbine utilized, the cross-sectional area is computed by multiplying the height of the turbine by the diameter of the turbine [19]. Equation 3 gives the amount of electrical power generated.

$$P_{MC} = \frac{1}{2} \cdot \rho \cdot C_p \cdot A \cdot v^3 \quad (3)$$

P_{MC} is the power produced by a marine current turbine in the case (Watt). ρ is the seawater's density (1025 kg/m³). The power coefficient is C_p (value is 0.35). The area proportion of the fluid flow's final power is represented by the value of C_p . A is the square footage per turbine in m², while v is the marine current's speed in m/s.

3.2 Solar Photovoltaic Generator

The regions in equator, such as in Indonesia are favorable place for generating electricity using solar photovoltaic (PV) [18]. Solar PVs can be placed in parallel or series [20]. Based on the radiation intensity or insolation, a photovoltaic systems produce electricity in formula as follows Equation 4 [21].

$$P_{PV} = \eta \cdot A \cdot S (1 - 0.005 (T_a - 25)) \quad (4)$$

Where η is the PV cells' efficiency of conversion, A is the PV surface's area in m², S is solar radiation (W/m²), and T_a is the surrounding air's temperature (in degrees Celsius). Solar PV has various types of materials, resulting in various conversion efficiencies. Solar PVs available in the market, in general, can be assumed having 15% conversion efficiency. Thus, every meter square of PV surface generates 150 Watt when receiving 1000 W/m² solar insolation.

Total power source (P_{TS}) Equation 5 is formulated by the arrangement of the marine current (P_{MC}), photovoltaic (P_{PV}), and battery power generation system [22].

$$P_{TS} = P_{MC} + P_{PV} \quad (5)$$

To calculate the total energy generated (E_{TS}) is found by multiplying each power in Equation 5 by each source operation time (t), as written as follows.

$$E_{TS} = P_{MC} \cdot t_{MC} + P_{PV} \cdot t_{PV} \quad (6)$$

The unit for energy produced is Watthour (Wh) or kWh. The operation time of the marine current denotes as t_{MC} . The availability of solar insolation in a day (t_{PV}), in equator region is typically 4.2 hours equivalent to the peak sun (at 1000 Watt/m²).

4. Battery Charge and Discharge

Battery characteristic, e.g. charge and discharge is necessary for system performance analysis [23]. A battery may hold the quantity of power is defined as follows Equation 7.

$$E_{bat,max} = Q_{bat} \cdot V \quad (7)$$

Where Q_{bat} is the battery's capacity (Ah), $E_{bat,max}$ is the maximum amount of energy the battery can store, and V is the battery's nominal voltage (Volt) [24]. The battery power meets the following Equation 8 criteria when it is being charged or discharged.

$$P_{Bat} = P_{TS} - P_L \quad (8)$$

When $P_{Bat} > 0$, the battery gets charged because there is excess power coming from the sources. The DC-to-DC Converter regulates the amount of power going into the battery [25]. However, if $P_{Bat} = 0$, it's possible that the sources won't be able to handle the loads, which will cause the battery to deplete.

4.1 Costing formula

The cost in this discussion is denoted by the letter C, and the unit cost by the letter U. The unit cost of power capacity, U_w (\$/ kW), multiplied by the power capacity installed, determines the cost of electricity generation (C_w) (P). This method determines how much it will cost to construct a power plant. Another approach of costing can be based on the energy produced. The generating cost (C_e) is calculated by multiplying the energy generated (E) by the energy generating cost unit, U_e (\$/kWh).

The following Equation 9 factors impact the price of a marine current power plant ($C_{W_{MC}}$).

$$C_{W_{MC}}(t) = U_{W_{MC}} \cdot P_{MC} \quad (9)$$

Similarly, the generating cost for photovoltaic is as follows Equation 10.

$$C_{W_{PV}} = U_{W_{PV}} \cdot P_{PV} \quad (10)$$

The battery cost is Equation 11.

$$C_{W_{Bat}} = U_{W_{Bat}} \cdot P_{Bat} \quad (11)$$

As a function of time, the entire cost of a marine current, PV, and battery system is as follows Equation 12.

$$C_{W_{Total}}(t) = C_{W_{MC}}(t) + C_{W_{PV}}(t) + C_{W_{Bat}}(t) \quad (12)$$

Each hour of the day's load demand patterns, along with the use of marine currents and PV generators, is used to determine the overall cost. It is expected that the total price includes the capital cost of all parts, including converters, installation, etc. According to energy calculation, the whole cost of generating energy is calculated as follows Equation 13.

$$C_{eTotal}(t) = C_{eMC}(t) + C_{ePV}(t) + C_{eBat}(t) \tag{13}$$

The unit cost of the marine current energy generation is represented as $U_{eMC} = 0.56 \text{ \$/kW}$, the PV power unit cost is $U_{WPV} = 300 \text{ \$/kW}$, and the battery unit cost is $U_{eBat} = 132 \text{ \$/kWh}$. The following Equation 14 relationship can be used to convert the unit cost of energy production U_e to the unit cost of power production U_w .

$$U_w = U_{eBat} \cdot 8760 \tag{14}$$

Assuming that the system is active every day of the year, 24 hours a day.

5. Results and Discussion

The proposed system was created with an area in Eastern Indonesia, close to Sulawesi Island, in mind. Figure 3 depicts the location of the Cibalulu Strait. Data about the present speed are gathered for the entire usual month. For 30 days, the data is shown hourly.



Figure 3 The location of Cibalulu Strait

Figure 4 depicts the daily pattern of the Cibalulu marine current speed. It shows the speed in the first 5 days in a typical month of Cibalulu Strait. The peak speed occurs every 6 hours perday. The highest speed is in the morning and decreasing gradually till midnight. The pattern forms homogen from hour-to-hour and day-to-day in a month.

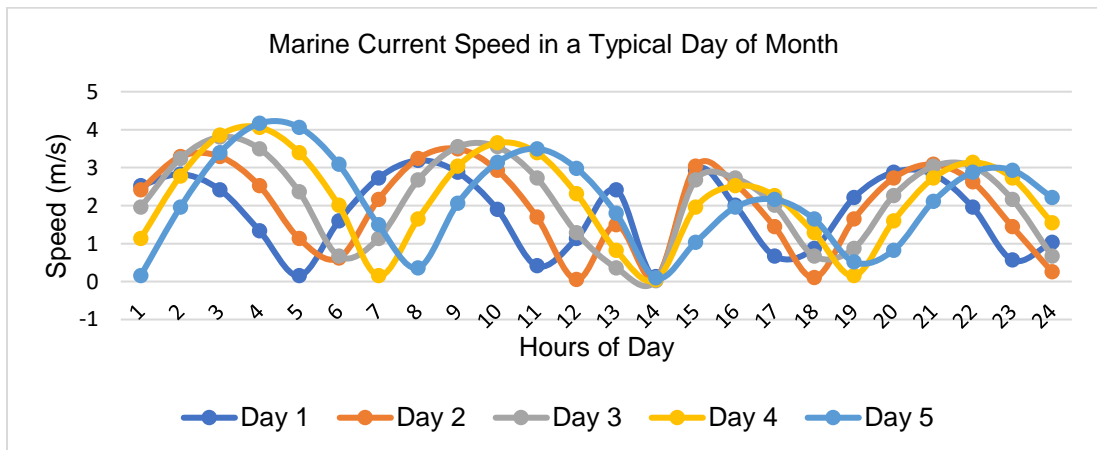


Figure 4. The Daily Pattern of Marine Current Speed at the First 5 Days of a Typical Month

The maximum speed perday for the whole typical month shows a sinusoidal waveform with period of 15 days, as illustrated in Figure 5. Thus, in the entire 31 days, it appears to be a two-cycle sinusoidal waveform. The first cycle has the maximum speed as 4.16 m/s and is reached, on day 6. At day 12, the valley's lowest speed is 2.4 m/s. The second

cycle begins on day 16 because there are two cycles in a month. Day 19 marks the second cycle's top speed, which is 4.42 m/s.

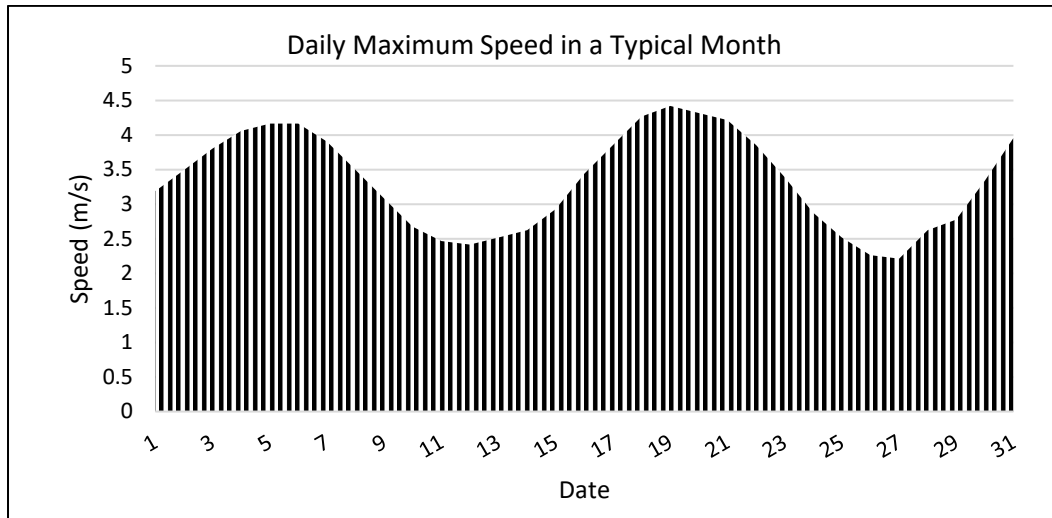


Figure 5. The Daily Maximum Speed of Marine Current in a Typical Month

Figure 6 illustrates the maximum and minimum speed in a typical day. The graph displays two curves, for instance, during a normal month's daily peak and lowest speed variations. Commonly, a sinusoidal waveform with four daily cycles results from the speed variation. The peak speed occurs every six hours or so. Early in the morning, a faster wave is appear, and it weakens throughout the day. The maximum speed in a typical month of the data sheet is discovered on day 19, when it is 4.4 m/s at 4:00 o'clock in the morning. The lowest speed is on day 27, when the maximum speed is 2.21 m/s at 18:00 o'clock.

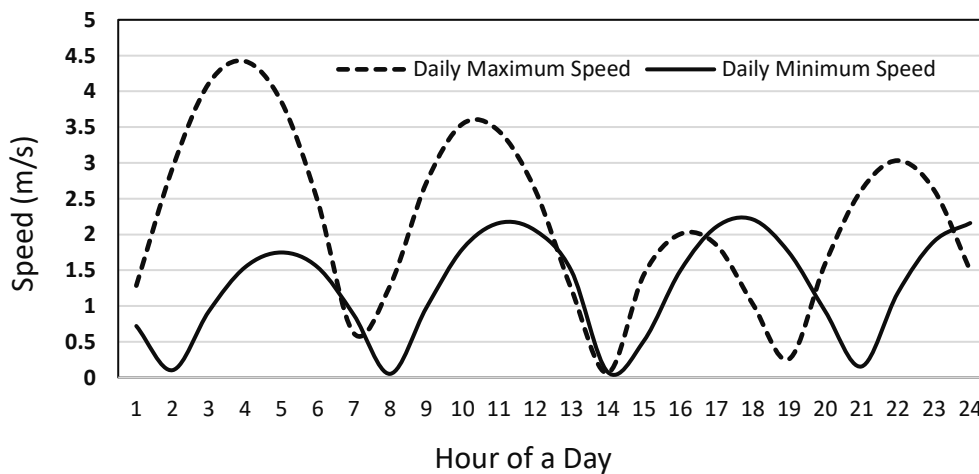


Figure 6 The Maximum and Minimum Speed in a Typical Day

The size of the marine turbine generator is determined using the presence data. The hourly load profile data and daily PV power generated are used in the calculation. The system is made to imitate running for a full month. Then, system component sizing optimization with the lowest cost as the result is carried out. The flowchart depicted in Figure 7 illustrates the optimization procedures. As can be seen, dynamic programming technique is used. In order to achieve the best power and cost, the dynamic programming technique uses a linear program that is simulated on Simulink matlab. A single 4.1 m-diameter turbine and a peak PV output of 60 kW, which requires 19 series and 17 parallel connections, are required for the best results. Battery having a 1030 kWh capacity.

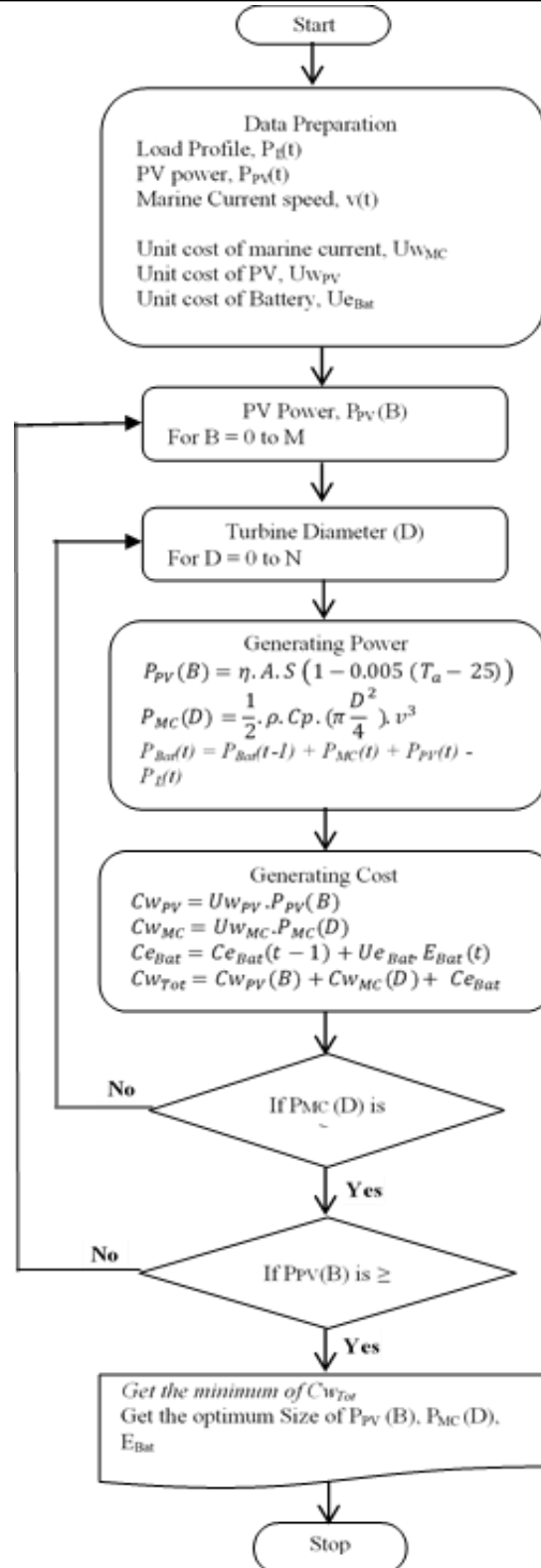


Figure 7. Dynamic Programming Flowchart for the Optimization

Each component's size is changed by a certain increment. All associated variables are then calculated. The diameter of the marine current is first determined, and the system is then used to operate for the greatest and minimum daily speeds, which happen on days 19 and 27, respectively.

Figure 8 shows the curves of excess power produced by the marine current generator vs the turbine radius, when running under daily maximum and minimum speeds. The curves are used to determine the optimum turbine radius and battery size considering the minimum system costs. These steps introduce the load-based battery discharge method. Initially, the turbine diameter is set without the presence of solar PV. A turbine with a radius of 1.8 meters can supply the load demand during the daily maximum speed, without any excess power. On the other hand, the turbine radius for balancing the power is found as 4.1 meters when the system operating under the lowest daily speed. Thus, an optimum turbine length can be placed between 1.8 meters and 4.1 meters, with additional battery storage. Solar PV may also include in the system that will contribute to reduce the battery size.

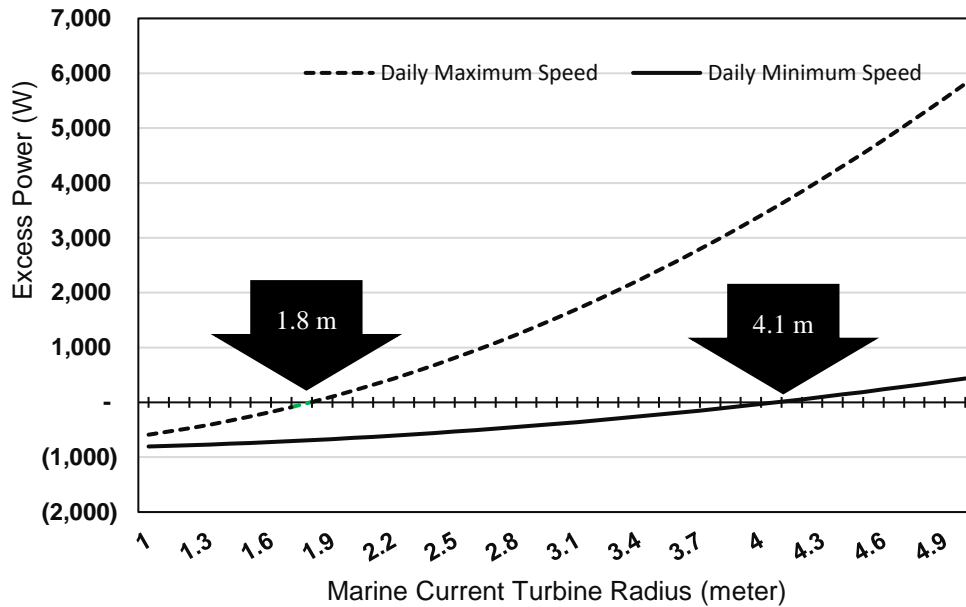


Figure 8. Turbine Radius and the Excess Power Produced

Figure 9 illustrates the battery balance cost as function of solar PV attached in the system. As can be seen, when 60 kW solar PV is installed, it provides the cheapest battery cost as USD\$ 2,157. This is matched when the radius of the marine current turbine is 4.1 meters.

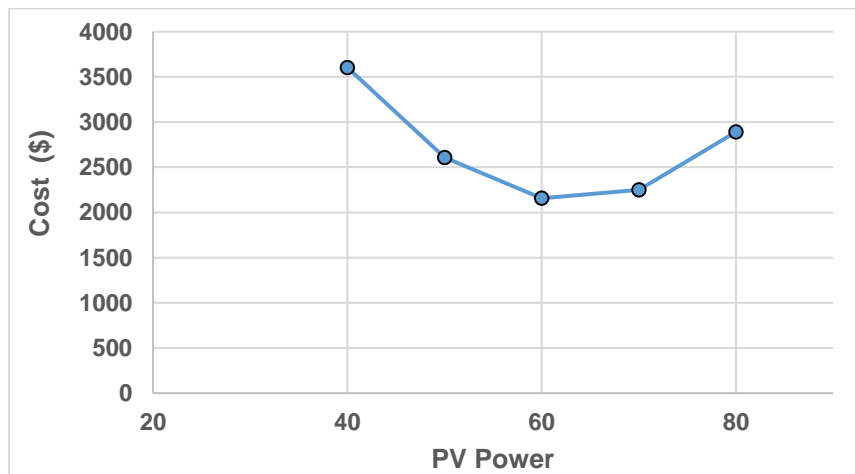


Figure 9 Cost of Battery Energy Balance

The total cost of energy generation to meet daily load requirements is shown in Table 3. It includes the prices for solar panels, batteries, and marine currents.

Table 3. The Daily Cost of Generating Power

Unit	Parameters	Value	Generating Cost (Ce)	Overall Cost (US\$)
Marine (4.1 m)	U_{WMC} (\$/kW)	3,900	56,9400	589,557
	P_{MC} (kW)	146		
PV (60)	U_{WPV} (\$/kW)	300	18,000	
	P_{PV} (kW)	60		
Baterai	U_{EBatt} (\$/kWh)	132	2,157	
	P_{Bat} (kWh)	16.34		

Figure 10 depicts the profiles when the sources are the optimum size, with the marine current's diameter being 4.1 meters and the PV power being 60 kW. The total energy is made up of four peaks from marine currents and one from solar PV energy.

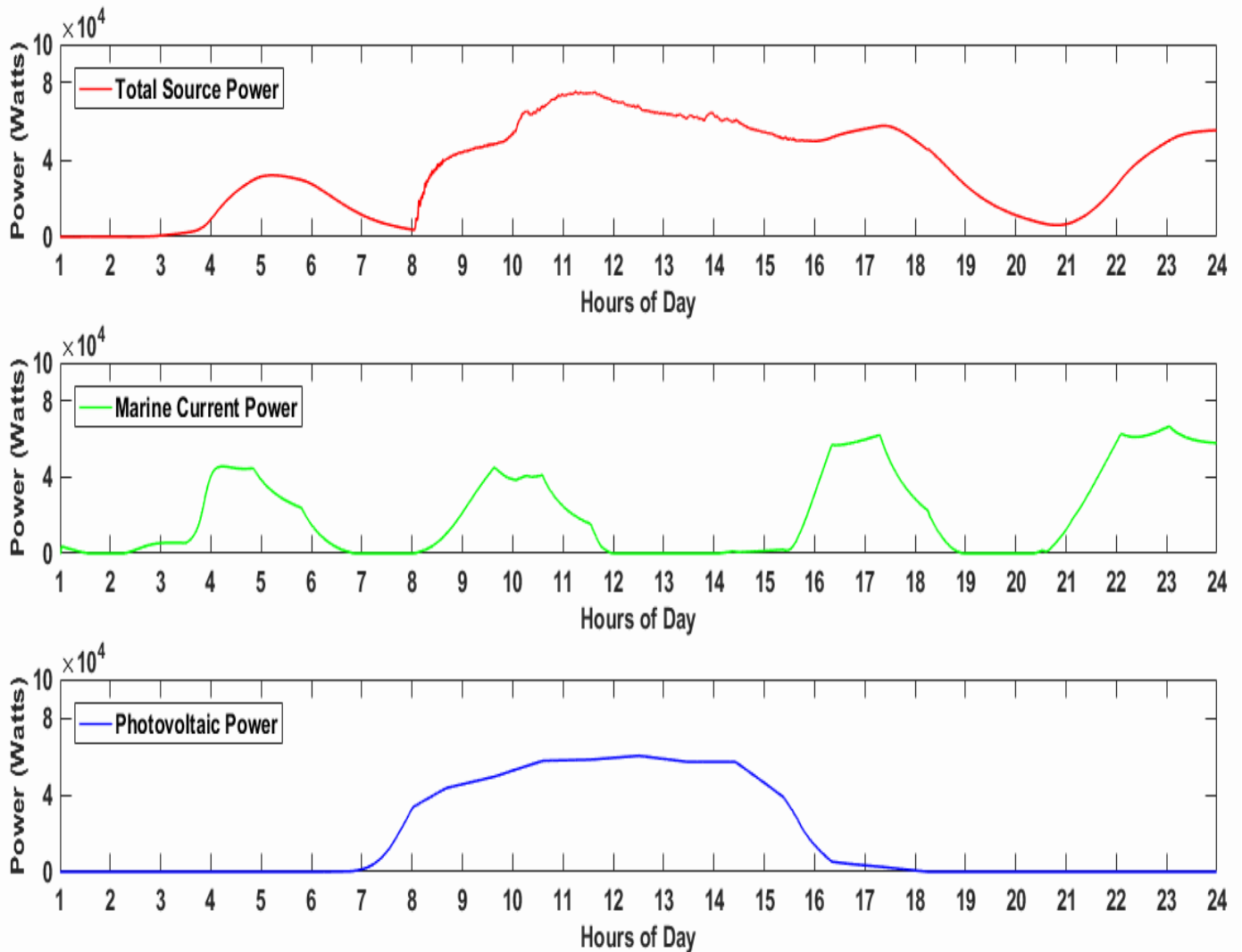


Figure 10. Electric Power from The Marine Current Turbines and the Photovoltaic

The curves for the total power source and the load profile are shown in Figure 11. The marine current generator matches the peak power, and the battery meets the energy need. The process of battery charging and draining determines the load needs. Ocean currents and solar PV energy sources are used to charge batteries. Depending on the battery's condition, charging can be completed within 24 hours. While the battery discharge is likewise carried out continuously over a 24-hour period. To satisfy the needs of the load, discharge is performed.

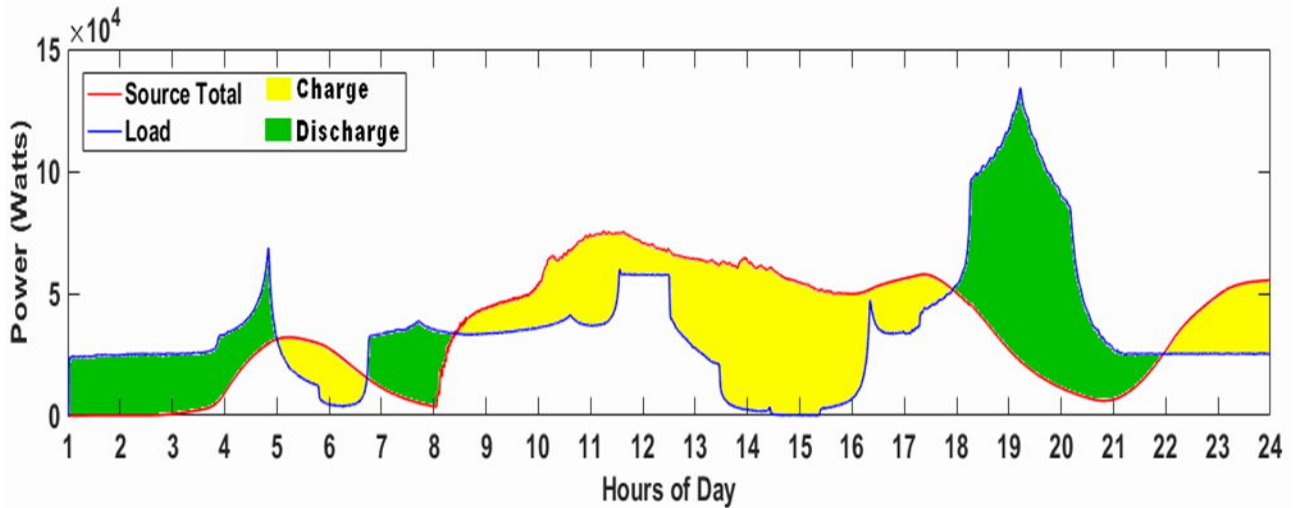


Figure 11. Power Matching Between the Sources and the Load Profile

The battery's state of charge can be used to observe the description of the charge and discharge operation (SOC). This procedure (SOC) is displayed as a percentage, showing the percentage of battery state over the course of a month. The rate of the marine currents, the load, and solar photovoltaic power all have an impact on this process.

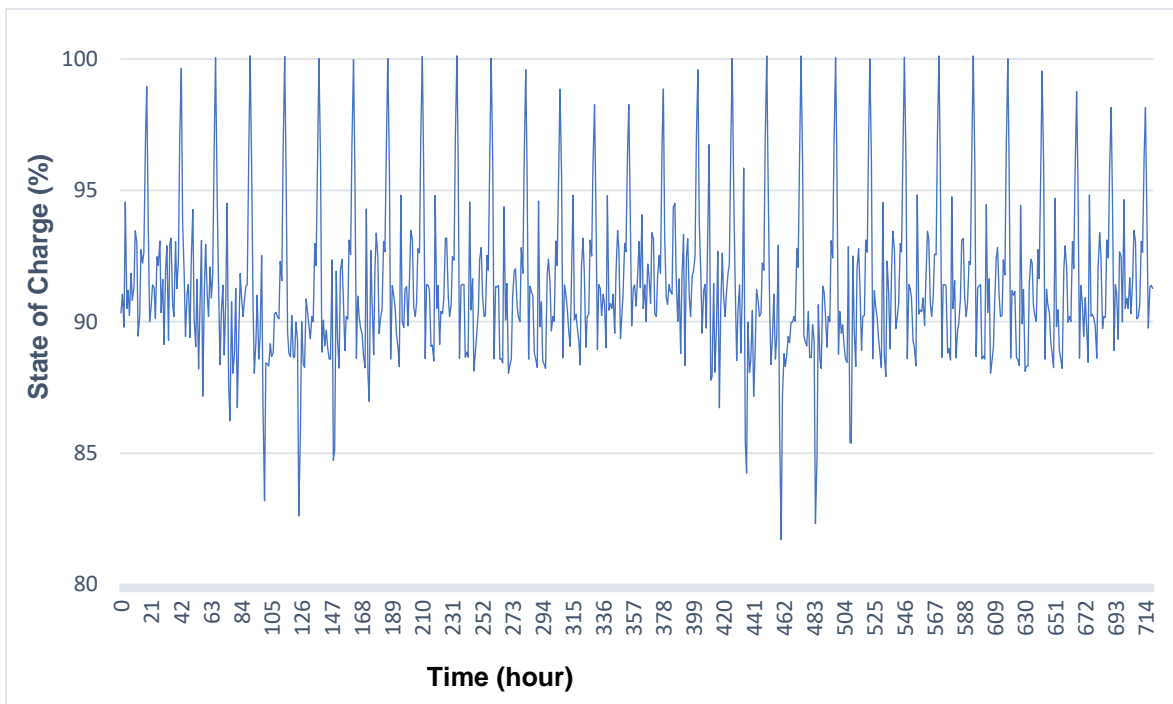


Figure 12. State of Charge of Battery in a Month

4. Conclusion

For the electricity of isolated small island, a hybrid system utilizing marine currents and solar PV with battery charge equilibrium was presented. The pattern is common for the settlements in Indonesia's Eastern Cibalulu Strait. The load that needs to be matched comprises six customer groups, a peak demand of 111.710 kW, and a daily energy consumption of 856.1 kWh. Using the dynamic programming with load-battery discharge method, sizing optimization was completed. The marine turbine's peak output was determined to be 146 kW, the PV system's maximum power was 60 kW, and the battery's capacity was 1030 kWh. As a result, the battery's state of charge (SOC) remains stable throughout the entire operation.

Acknowledgement

For granting us permission to use every facility in the laboratory, we would like to thank the head of the energy conversion laboratory at the Institute of Sepuluh November (ITS).

References

- [1] Faanzir, Soediby, and M. Ashari, "Emission abatement cost analysis of hybrid marine current/photovoltaic/diesel system operation," *Proc. - 2017 Int. Semin. Appl. Technol. Inf. Commun. Empower. Technol. a Better Hum. Life, iSemantic 2017*, vol. 2018-Janua, pp. 248–252, 2017. <https://doi.org/10.1109/ISEMANTIC.2017.8251878>
- [2] M. Z. Z. Muhtadi, Soediby, and M. Ashari, "Penetration of Photovoltaic-Synchronous Diesel Generator Systems without Storage for Isolated Area," 2019. <https://doi.org/10.1109/ICOMITEE.2019.8921203>
- [3] R. O. Pratama, M. Effendy, and Z. Zulfatman, "Optimization of Maximum Power Point Tracking (MPPT) Using P&O-Fuzzy and IC-Fuzzy Algorithms on Photovoltaic," *Kinet. Game Technol. Inf. Syst. Comput. Network, Comput. Electron. Control*, 2018. <https://doi.org/10.22219/kinetik.v3i2.200>
- [4] H. Zsiborács *et al.*, "Intermittent renewable energy sources: The role of energy storage in the european power system of 2040," *Electron.*, vol. 8, no. 7, 2019. <https://doi.org/10.3390/electronics8070729>
- [5] Z. W. J. Al-Shammari, M. M. Azizan, and A. S. F. Rahman, "Grid-independent pv-wind-diesel generator hybrid renewable energy system for a medium population: A case study," *J. Eng. Sci. Technol.*, vol. 16, no. 1, pp. 92–106, 2021.
- [6] A. Maimó-Far, A. Tantet, V. Homar, and P. Drobinski, "Predictable and unpredictable climate variability impacts on optimal renewable energy mixes: The example of Spain," *Energies*, vol. 13, no. 19, 2020. <https://doi.org/10.3390/en13195132>
- [7] J. Olmedo-González, G. Ramos-Sánchez, E. P. Garduño-Ruiz, and R. de G. González-Huerta, "Analysis of Stand-Alone Photovoltaic—Marine Current Hybrid System and the Influence on Daily and Seasonal Energy Storage," *Energies*, vol. 15, no. 2, 2022. <https://doi.org/10.3390/en15020468>
- [8] D. Parra *et al.*, "An interdisciplinary review of energy storage for communities: Challenges and perspectives," *Renew. Sust. Eerg. Rev.*, vol. 79, no. March, pp. 730–749, 2017. <https://doi.org/10.1016/j.rser.2017.05.003>
- [9] Asian Development association, *Handbook on Battery Energy Storage System*, no. December. 2018.
- [10] T. Taufik, "The DC House project: An alternate solution for rural electrification," *Proc. 4th IEEE Glob. Humanit. Technol. Conf. GHTC 2014*, pp. 174–179, 2014. <https://doi.org/10.1109/GHTC.2014.6970278>
- [11] R. Weiss, L. Ott, and U. Boeke, "Energy efficient low-voltage DC-grids for commercial buildings," 2015. <https://doi.org/10.1109/ICDCM.2015.7152030>
- [12] S. H. Song, S. Il Kang, and N. K. Hahm, "Implementation and control of grid connected AC-DC-AC power converter for variable speed wind energy conversion system," in *Conference Proceedings - IEEE Applied Power Electronics Conference and Exposition - APEC*, 2003, vol. 1. <https://doi.org/10.1109/APEC.2003.1179207>
- [13] O. Lopez-Santos, "Contribution to the DC-AC conversion in photovoltaic systems: Module oriented converters," *Citeseer*, 2015. <https://doi.org/10.13140/RG.2.1.3400.3368>
- [14] S. Kolsi, H. Samet, and M. Ben Amar, "Design Analysis of DC-DC Converters Connected to a Photovoltaic Generator and Controlled by MPPT for Optimal Energy Transfer throughout a Clear Day," *J. Power Energy Eng.*, vol. 02, no. 01, 2014. <http://dx.doi.org/10.4236/jpee.2014.21004>
- [15] G. D. P. da Silva and D. A. C. Branco, "Modelling distributed photovoltaic system with and without battery storage: A case study in Belem, northern Brazil," *J. Energy Storage*, vol. 17, 2018. <https://doi.org/10.1016/j.est.2018.02.009>
- [16] J. Eum and Y. Kim, "Analysis on operation modes of residential BESS with balcony-PV for apartment houses in Korea," *Sustain.*, vol. 13, no. 1, 2021. <https://doi.org/10.3390/su13010311>
- [17] P. Fairley, "DC versus AC: The second war of currents has already begun [in my view]," *IEEE Power and Energy Magazine*, vol. 10, no. 6, 2012. <https://doi.org/10.1109/MPE.2012.2212617>
- [18] F. N. Budiman and M. R. Ramadhani, "Total Harmonic Distortion Comparison between Sinusoidal PWM Inverter and Multilevel Inverter in Solar Panel," *Kinet. Game Technol. Inf. Syst. Comput. Network, Comput. Electron. Control*, 2018. <https://doi.org/10.22219/kinetik.v3i3.617>
- [19] F. Novico, E. H. Sudjono, A. Egon, D. Menier, M. Methew, and M. B. Pratama, "Tidal current energy resources assessment in the patinti strait, indonesia," *Int. J. Renew. Energy Dev.*, vol. 10, no. 3, pp. 517–525, 2021. <https://doi.org/10.14710/ijred.2021.35003>
- [20] N. B. M. Yusof and A. Bin Baharuddin, "The study of output current in photovoltaics cell in series and parallel connections," *Int. J. Technol. Innov. Humanit.*, vol. 1, no. 1, pp. 7–12, 2020. <https://doi.org/10.29210/88701>
- [21] N. Odkhuu, K. B. Lee, M. A. Ahmed, and Y. C. Kim, "Optimal energy management of V2B with RES and ESS for peak load minimization," *Appl. Sci.*, vol. 8, no. 11, 2018. <https://doi.org/10.3390/app8112125>
- [22] Faanzir, Soediby, and M. Ashari, "Optimum sizing of marine current/PV/battery hybrid power system for isolated island minigrd," in *Proceedings - 2017 International Seminar on Application for Technology of Information and Communication: Empowering Technology for a Better Human Life, iSemantic 2017*, 2017, vol. 2018-January. <https://doi.org/10.1109/ISEMANTIC.2017.8251875>
- [23] I. U. vistalina Simanjuntak, H. Heryanto, Y. Rahmawaty, and T. Manurung, "Performance Analysis of VRLA Battery for DC Load at Telecommunication Base Station," *ELKHA*, vol. 13, no. 2, 2021. <http://dx.doi.org/10.26418/elkha.v13i2.49202>
- [24] Z. Šimić, G. Knežević, D. Topić, and D. Pelin, "Battery energy storage technologies overview," *International Journal of Electrical and Computer Engineering Systems*, vol. 12, no. 1. 2021. <https://doi.org/10.32985/ijeces.12.1.6>
- [25] J. D. Paez, D. Frey, J. Maneiro, S. Bacha, and P. Dworakowski, "Overview of DC-DC Converters Dedicated to HVdc Grids," *IEEE Trans. Power Deliv.*, vol. 34, no. 1, 2019. <https://doi.org/10.1109/TPWRD.2018.2846408>